Published in final edited form as:
Biol Psychiatry. 2015 February 1; 77(3): 266–275. doi:10.1016/j.biopsych.2014.06.024.

In vivo ketamine-induced changes in [^{11}C]ABP688 binding to metabotropic glutamate receptors subtype 5

Christine DeLorenzo, PhD[1,2,6], **Nicole DellaGioia, MA**[7], **Michael Bloch, MD**[7,10], **Gerard Sanacora, MD, PhD**[7], **Nabeel Nabulsi, PhD**[8], **Chadi Abdallah, MD**[7,11], **Jie Yang, PhD**[4], **Ruofeng Wen, BA**[5], **J. John Mann, MD**[6], **John H. Krystal, MD**[7,11], **Ramin V. Parsey, MD, PhD**[1,3], **Richard E. Carson, PhD**[8,9], and **Irina Esterlis, PhD**[7,10]

[1]Department of Psychiatry, Stony Brook University

[2]Department of Biomedical Engineering, Stony Brook University

[3]Department of Radiology, Stony Brook University

[4]Department of Preventive Medicine, Stony Brook University

[5]Department of Applied Mathematics and Statistics, Stony Brook University

[6]Columbia University Department of Psychiatry

[7]Department of Psychiatry, Diagnostic, Yale University

[8]Department of Radiology, Biomedical, Yale University

[9]Department of Engineering, Yale University

[10]Department of Child Study Center, Yale University

[11]Clinical Neuroscience Division, VA National Center for PTSD

Corresponding Author Address: Christine DeLorenzo Stony Brook University Department of Psychiatry HSC-T10-040D Stony Brook, NY 11794 Phone: 631-638-1523 Fax: 631-444-1560 Christine.DeLorenzo@stonybrookmedicine.edu.

Financial Disclosures:

Dr. Mann receives royalties for commercial use of the C-SSRS from the Research Foundation for Mental Hygiene and has stock options in Qualitas Health a start-up company working on an EPA nutritional product. CGA received a research fund or consultation fee from Genentech. John Krystal consults for several pharmaceutical and biotechnology companies, with compensation less than $10 000 per year. These companies include AbbVie, Inc.; Amgen; Astellas Pharma Global Development; AstraZeneca Pharmaceuticals; Biomedisyn Corporation; Bristol-Myers Squibb; Easton Associates; Eli Lilly and Co.; F. Hoffman-L Roche Ltd; Forest Laboratories; Gilead Sciences, Inc.; GlaxoSmithKline; Janssen Research & Development; Novartis; Otsuka Pharmaceutical, Development & Commercialization, Inc.; Sage Therapeutics, Inc.; Shire Pharmaceuticals; Sunovion Pharmaceuticals, Inc.; Takeda Industries. Dr Krystal is a member of the following scientific advisory boards: CHDI Foundation, Inc.; Lohocla Research Corporation, Mnemosyne Pharmaceuticals, Inc.; Naurex, Inc.; and Pfizer Pharmaceuticals. In addition, Dr Krystal is a past president of the American College of Neuropsychopharmacology, editor of Biological Psychiatry; and an employee of the Yale University School of Medicine and the VA CT Health System. He is an originator on the following patent: Seibyl JP, Krystal JH, and Charney DS; Dopamine and noradrenergic reuptake inhibitors in treatment of schizophrenia; Patent #:5 447 948; 5 September 1995. In addition, he is an originator of the following relevant pending patents: (1) Vladimir, Coric; Krystal, John H, Sanacora, Gerard—Glutamate Agents in the Treatment of Mental Disorders No 11/399 188; 5 April 2006 (Pending). (2) Intranasal Administration of Ketamine to Treat Depression (Pending). All other authors report no biomedical financial interests or potential conflicts of interest.

Abstract

Background—At subanesthetic doses, ketamine, an *N*-Methyl-D-aspartate (NMDA) glutamate receptor antagonist, increases glutamate release. Here, we imaged the acute effect of ketamine on brain metabotropic glutamatergic receptors subtype 5 (mGluR5) with a high affinity PET ligand [^{11}C]ABP688 ((E)-3-((6-methylpyridin-2-yl)ethynyl)-cyclohex-2-enone-*O*-^{11}C-methyl-oxime), a negative allosteric modulator of mGluR5.

Methods—Ten healthy nonsmoking human volunteers (34±13 years old) received two [^{11}C]ABP688 PET scans on the same day – before (scan 1) and during i.v. ketamine administration (0.23mg/kg over 1min, then 0.58mg/kg over 1h; scan 2). PET data were acquired for 90 min immediately following [^{11}C]ABP688 bolus injection. Input functions were obtained through arterial blood sampling with metabolite analysis.

Results—A significant reduction in [^{11}C]ABP688 volume of distribution (V_T) was observed in scan 2 relative to scan 1 of 21.3 ± 21.4%, on average, in the anterior cingulate, medial prefrontal cortex, orbital prefrontal cortex, ventral striatum, parietal lobe, dorsal putamen, dorsal caudate, amygdala, and hippocampus. There was a significant increase in measurements of dissociative state after ketamine initiation ($p<0.05$) that resolved after completion of the scan.

Discussion—This study provides first evidence that ketamine administration decreases [^{11}C]ABP688 binding *in vivo* in human subjects. Results suggest that [^{11}C]ABP688 binding is sensitive to ketamine-induced effects, although the high individual variation in ketamine response requires further examination.

Keywords

ketamine; PET; [^{11}C]ABP688; glutamate; mGluR5; brain

Introduction

Glutamate, the principal excitatory neurotransmitter, is found throughout the brain, and alterations in the glutamatergic system have been implicated in variety of disorders, including addiction (1-3), major depressive disorder (MDD) (4-6), and bipolar disorder (BD) (7). Glutamate may contribute to abnormalities in sleep, appetite, motivation, and concentration (8). Altering the glutamatergic system may thus lead to improvements in functioning, and glutamatergic agents are being actively evaluated as potential rapidly acting antidepressants (9-12).

The noncompetitive *N*-Methyl-D-aspartate (NMDA) glutamate receptor antagonist, ketamine, has been extensively studied for its capacity to produce a rapid antidepressant response (within 4-24 hrs) in treatment-resistant depression (11, 13-17). The neurobiology underlying the antidepressant effects of ketamine is being explicated by current research. Perhaps as a consequence of its ability to reduce the recruitment of GABA interneurons, administration of subanesthetic ketamine doses stimulate or disinhibit cortical glutamate release, as measured in rodents with *in vivo* microdialysis (18, 19) and magnetic resonance spectroscopy (20) (^{13}CMRS) and in humans with magnetic resonance spectroscopy (21) (^{1}H-MRS). Improving our understanding of the cascade of events that occur after glutamate

release is necessary to provide insight into the mechanism of action of ketamine. For example, glutamate release produced by ketamine stimulates -amino-3-hydroxy-5-methyl-4-isoxazolepropionic acid (AMPA) receptors, enhancing downstream signaling mechanisms, such as the mammalian target of rapamycin (mTOR) pathway (22). Enhanced signaling rapidly increases dendritic spine production, reversing deficits in spines associated with the unpredictable stress model in rats (23). The disinhibition in cortical networks produced by ketamine is reflected in increased resting state cortical functional connectivity, as measured with functional MRI (24, 25). However, much is still unknown about the downstream effects at other glutamate receptors.

The purpose of the current study was to explore whether increases in glutamate release produced by ketamine administration in humans would be reflected in reductions in ligand binding to metabotropic glutamatergic receptors (mGluR5). Generally speaking, there are parallels between the proposed approach and paradigms employed to characterize changes in neurotransmitters such as GABA, acetylcholine, and dopamine release in psychiatric illness and other diseases (26-30). In those cases, the radioligand and the neurotransmitter bind to the same site. However, the available ligands for measurement of mGluR5 using positron emission tomography (PET) ([^{18}F]FPEB (31, 32), [^{11}C]ABP688 (4, 33-35), and [^{11}C]SP203 (36)) are negative allosteric modulators (NAMs). Therefore, in contrast to previous studies, the current study explores the hypothesis that glutamate released during the infusion of ketamine, a drug that does not bind to mGluR5 with high affinity, would reduce [^{11}C]ABP688 binding to mGluR5 through mechanisms other than direct competition.

Methods and Materials

Subjects

This study was approved by the Yale University Institutional Review Board and Radiation Safety Committee and by the Yale-New Haven Hospital Radiation Safety Committee. After completing the informed consent process, inclusion criteria were assessed by the following: physical, routine blood tests, psychiatric and neurological examination. A urine drug screen, ECG, and a pregnancy test (for women) were performed at screening and before radiotracer administration. General inclusion criteria were: 1. Subjects are between 18 and 60 years old, 2. English speaking, 3. No current, or history of, any DSM-IV diagnosis, 4. No first-degree relative with history of psychotic, mood, or anxiety disorder, 5. No recent regular medication use, and no history of psychiatric medication use. Thirteen subjects were deemed eligible to participate in the study. Of those, one subject was withdrawn from the study after the baseline PET scan due to high blood pressure (prior to ketamine administration); two could not tolerate the full ketamine dose and were unable to continue with the scanning procedures, thus their data was discarded. In total, ten healthy non-smoking volunteers (5 males, 5 females) completed this study (mean age: 33.5 ± 13.2 years).

Psychiatric Assessments

Psychiatric history and a structured clinical interview (SCID-NP) were conducted at screening. The Hamilton Rating Scale for Depression (HAM-D 29) (37), Montgomery–Åsberg Depression Rating Scale (MADRS) (38), and Beck Depression Inventory (BDI) (39)

were used to assess subjects' depressive symptoms during intake and on PET scan day (before and 30 min and 24 hours after ketamine administration). The effects of ketamine on the subject's mental state were subjectively assessed using the Clinician Administered Dissociative State Scale (CADSS) (40) and Profile of Mood States (POMS) (41).

Positron Emission Tomography

High specific activity [^{11}C]ABP688 (1073 ± 370 MBq/nmol at EOS) was produced from the reaction of [^{11}C]methyl iodide with desmethyl-ABP688 using the loop method developed by Nabulsi (42). The average radiochemical and chemical purities were 97% (n = 20). The average *E/Z* isomer ratio in the final PET drug product was 70:1 (by analytical radio HPLC area percent, with *E* being the major isomer). The *E*-isomer has been shown to exhibit a higher K_D *in vivo* (43). PET imaging was performed on a High-Resolution Research Tomograph (HRRT, Siemens, Knoxville, TN). A 6 min transmission scan was acquired before injection. [^{11}C]ABP688 was then administered as a bolus over 1 min and emission data were collected for 90 min in list mode. (Ninety minutes of data were collected in case 60 min were not sufficient to capture ketamine-induced effects. However, due to the rapid effects of ketamine, this was not the case.) Sixty min of list-mode data were used, binned into 14 frames (6 at 30 sec, 3 at one min, 2 at 2 min, and 10 at 5 min duration), based on previous analysis with this tracer that indicated that 60 min is sufficient (44, 45). Head motion was recorded during the scan using a commercial optical tracking system, the Polaris Vicra system (Northern Digital Inc., Waterloo, ON, Canada). Images were reconstructed and corrected for attenuation, scatter, and motion using the MOLAR algorithm (46).

Following the baseline [^{11}C]ABP688 scan, subjects were given a short (~ 1 hour) break and then received the ketamine challenge scan. A second [^{11}C]ABP688 dose was administered over 1 min and then ketamine was administered immediately after successful radioligand administration. This design was used in order to decrease subject burden in case of equipment failure, and to ensure capture of the immediate effects of ketamine, given that it induces a rapid glutamate release. Vital signs (pulse, blood pressure, and SPO_2) were obtained before and after ketamine administration, and during the ketamine infusion (at 5-10 min intervals).

Racemic ketamine was obtained from the Yale New Haven Hospital Pharmacy and administered intravenously, as previously described (47, 48) (initial bolus of 0.23 mg/kg over 1 min followed by constant infusion of 0.58 mg/kg per hour over 1 hour). This is a subanesthetic but psychotomimetic dose. This dosing regimen of ketamine was used, instead of the usual antidepressant dosing of 0.5 mg/kg over 40 min, to enhance statistical power by inducing a larger glutamate surge as suggested by prior ketamine studies (49-51). Both dosing regimens are similar in the fact that they result in comparable changes in cognition and perception but do not cause the anesthetic effect. At 5, 15, 30, and 75 minutes, blood ketamine levels were assessed, as previously described (48), in all subjects except for #10 (venous blood samples for ketamine analysis could not be drawn after study initiation).

In order to perform delineation of anatomical regions on the PET data, images were coregistered with T1-weighted Magnetic Resonance Images (MRIs) acquired on a 3T Trio

imaging system (Siemens Medical Systems, Erlangen, Germany) with a voxel size of 1 × 1 × 1 mm.

Input Function Measurement

Prior to PET imaging, catheters were inserted in the radial artery and forearm veins for arterial blood sampling and radioisotope injection, respectively. Blood activity was measured continuously for the first 7 min after radiotracer administration, and manually at 2, 4, 9, 12, 15, 20, 25, 30, 40, 50, and 60 min. Radioactivity was analyzed as described previously (52). After correction for delay and dispersion as previously described (53), the automated and manual plasma concentration values were merged and smoothed by convolution with a Gaussian function (FWHM = 24 s).

An HPLC assay of five of the arterial blood samples (at 0, 4, 12, 30, and 60) was used to establish unmetabolized parent compound levels (54). Unmetabolized parent fraction levels were fitted with a Hill function, which is described by three parameters (A, B, and C), in which percent parent compound = $A*(t^B/[t^B+C]) + 1$, where t is time (55). The input function was calculated as the product of the interpolated parent fraction and the merged plasma counts. This combined data was then fitted as the combination of a straight line and the sum of three exponentials, describing the function before and after the peak, respectively, resulting in the metabolite-corrected arterial input function. Free fraction (f_P) measurements were performed using an ultrafiltration technique (54). However, all measured free fraction values were < 3% and considered unreliable, as has been shown previously (44).

Image Analysis

Image analysis was performed using MATLAB (The MathWorks, Natick, MA). Subsequent frames of each PET study were registered to the eighth frame using the FMRIB linear image registration tool (FLIRT), version 5.0 (FMRIB Image Analysis Group, Oxford, UK), to correct for residual subject motion that may not have been accounted for by the Polaris Vicra system. Probabilistic regions of interest were determined using nonlinear registration techniques as previously described (56). The mean PET image was then coregistered to the subject's MRI using a semi-automated technique (57). Time activity curves were generated from the mean of the measured activity, weighted by regional label probabilities, within a region over the time course of the PET acquisition.

Outcome Measure Calculation

Regional outcome measures were calculated using an unconstrained two-tissue compartment (2TC) model, as previously validated for this tracer (45). For computational efficiency, the Logan graphical approach was used for voxel analysis (58). Given the unreliable f_P values and lack of a reference region (59), V_T (volume of distribution: ratio of the concentration of the ligand in the region of interest to that in the plasma at equilibrium (60)) was used as the outcome measure. Percent change in radioligand binding was calculated as $[(V_{T,baseline}-V_{T,ketamine}) / V_{T,baseline}]*100$.

Statistical Analysis

To determine the significance of detected binding differences due to ketamine administration, a linear mixed-effects model with region as a fixed effect was applied to the data. The dependence structure among regions and scans from the same subject was modeled using the Kronecker product between unrestricted symmetry (to model the correlation among all regions) and compound symmetry (to model the correlation between two scans). The interaction term between region and scan was examined and removed from the model if appropriate. Linear mixed models for longitudinal data were also used to model change in patients' vital signs after ketamine administration. The dependence structure used in these models was compound symmetry. The paired comparisons of scores from subjective reports from two time points were carried out through Wilcoxon's signed rank test. Both unadjusted p-values and False Discovery Rate (FDR) corrected values, based on Benjamini & Hochberg method, were reported for these paired comparisons. All tests were two-sided and all analyses were carried out using R 3.0.2 (http://www.r-project.org/) and SAS 9.3 (SAS Institute Inc., Cary, NC).

Results

Vital Signs/Subjective Report

On average, there was a significant increase in heart rate and blood pressure after start of ketamine (compared to baseline, Table 1). After 30 minutes, both heart rate and blood pressure had mostly returned to baseline levels. SPO_2 levels remained relatively constant.

Significant changes in Clinician Administered Dissociative State Scale (CADSS) scores were observed. Baseline values (acquired prior to scan 1) were 0 for all subjects, except Subject 2, who reported a value of 1 for the CADSS 12 and derealization subscale. Subjects scored significantly higher on many CADSS subscales during ketamine as compared to baseline (Figure 1). There were no significant differences between scores at baseline and study end (60 min post ketamine). There were no significant differences in the POMS, BDI, or MADRS scores during the ketamine challenge compared to baseline. (The HAM-D was only collected at baseline for most subjects, Table 2.)

Tracer Metabolism/Clearance

There were no significant differences between scans (scan 1, scan 2, *p*-value) in the injected dose (576±136MBq, 593±116MBq, 0.63), specific activity (215.2 ± 194.4 MBq/nmol, 246.4 ± 224.2 MBq/nmol, 0.56) or mass (1.1 ± 0.7 μg, 1.2 ± 1.0 μg, 0.85). To assess the potential effects of ketamine on tracer metabolism, the fitted average unmetabolized parent compound curves were evaluated before and after the ketamine infusion. Two of the three parameters (A and B, see Input Function Measurement) used to fit the subjects' metabolite values were significantly different post-ketamine versus pre-ketamine ($p = 0.02$ in both cases) indicating a potential ketamine-induced slowing of metabolism or tracer clearance. Further, when the delivery rate of the [^{11}C]ABP688 from arterial plasma to the tissue was examined (K_1 (60)), significant increases in this parameter were observed in a region dependent manner ($p = 0.018$, linear mixed effects model). However, clearance values, calculated as the injected dose divided by the extrapolated area under the metabolite-corrected arterial input function

(61), were not significantly different across scans (baseline: 99.3 ± 32.2 L/h, ketamine: 90.1 ± 27.7 L/h, $p = 0.23$).

Ketamine-Induced Change in [^{11}C]ABP688 Binding

A significant reduction in [^{11}C]ABP688 binding was observed qualitatively and quantitatively (Figures 2 and 3). [^{11}C]ABP688 binding (V_T) significantly decreased in a region-dependent manner after ketamine administration, as compared to the baseline scan (all region-specific $p < 0.007$, linear mixed effects model, including all brain regions in Figure 3) (Figures 2-4). On average, there was a 21.3% decrease in regional V_T after ketamine across all regions and subjects. The average ketamine-induced change in V_T (across all subjects) was 20±23% in the anterior cingulate (Figure 4a), 20±22% in the medial prefrontal cortex (Figure 4b), 20±22% in the orbital prefrontal cortex, 20±22% in the ventral striatum (Figure 4c), 21±20% in the parietal lobe, 22±21% in the dorsal putamen, 20±22% in the dorsal caudate (Figure 4d), 25±21% in the amygdala (Figure 4e) and 22±20% in the hippocampus. Similar to the high binding regions, the cerebellum showed high variability in binding change (average binding decrease: 16.4% ± 18.8%, range: 42.4% decrease to 14.1% increase, Figure 4f). The red lines in Figure 4 indicate the change in average regional V_T after ketamine administration.

Blood ketamine levels were variable, with averages (over the first 30 min) ranging from 82 ± 65 ng/mL to 202 ± 30 ng/mL. No significant correlations were observed between CADSS subscores (average, amnesia, depersonalization, or derealization) and ketamine levels. Further, no significant correlations were observed between CADSS subscores, or total injected amount of ketamine or ketamine concentration in blood, and average V_T percent change.

Discussion

The goal of this study was to develop a paradigm to measure ketamine-induced changes in mGluR5 availability as an index of glutamate release using PET and [^{11}C]ABP688. We provide first evidence that ketamine administration decreases [^{11}C]ABP688 binding *in vivo* in human subjects. Increases in heart rate, blood pressure and self-report on a questionnaire of dissociative symptoms were in line with ketamine effects.

We observed a global reduction of ~20% in [^{11}C]ABP688 binding with ketamine administration. It is conventional to compare such changes to that measured in test/retest scans. Using a test/retest design, preclinical literature shows excellent reproducibility of [^{11}C]ABP688 binding (5-10% (34, 44, 62)) although human studies are less consistent (33, 35). Burger et al. (35) found high reproducibility between bolus and bolus/infusion studies in five healthy male volunteers scanned a few weeks apart (average percent difference <1%). However, we reported an *increase* (19.7%, on average) in [^{11}C]ABP688 binding during the second (same day afternoon) scan of a bolus test/retest paradigm (33). It is important to note that, in the current study, the average binding *decreased* in the second (ketamine) scan. Thus, this effect is therefore likely not attributable to tracer binding variability, and could potentially be underestimated because of the test-retest effects we previously reported.

In this study, changes in V_T, which include both specific and nonspecific binding, were measured. It was not possible to directly measure specific binding, since a region devoid of mGluR5 receptors in the human brain does not exist; therefore, there is no reference region to be used for this ligand (44, 63, 64). Without a true estimate of the nondisplaceable binding (V_{ND}), specific binding potential (BP_P or BP_{ND}) cannot be reliably estimated directly. We therefore estimated BP_{ND} using a previously described technique (data not shown). Kagedal and colleagues (64) administered an mGluR5 negative allosteric modulator (AZD6200) to healthy human subjects and used a nonlinear mixed effects model to simultaneously estimate mGluR5 occupancy and nondisplaceable binding in the cerebellum. By fixing the ratio of cerebellar nonspecific to specific binding to that estimated by Kagedal et al (1.33), we estimated V_{ND} from baseline images and used it to estimate BP_{ND} (in the baseline and ketamine images). Using this estimate, as expected, percentage changes in [^{11}C]ABP688 BP_{ND} were slightly larger than those observed using V_T with evidence of a scan by region interaction (anterior cingulate 28±30%, medial prefrontal cortex 29±31%, orbital prefrontal cortex 29±31%, ventral striatum 29±30%, parietal lobe 30±29%, dorsal putamen 32±30%, dorsal caudate 30±33%, amygdala 38±30% and hippocampus 34±29%, all region-specific $p < 0.001$, based on the linear mixed effects model).

Results indicate that [^{11}C]ABP688 V_T decreased in all brain regions. Given that [^{11}C]ABP688 and glutamate bind at different sites on the receptor, this decrease should not be due to direct competition. However, the mechanism responsible for the change in [^{11}C]ABP688 binding is not clear. Previously, it was shown that N-acetylcysteine (NAC) administration to baboons, which raises extrasynaptic glutamate levels through activating the cystine-glutamate antiporter, reduced [^{11}C]ABP688 binding (10-20% of BP_{ND}) (34). The authors hypothesized that the decrease in BP_{ND} (proportional to the affinity of the radiotracer for the binding site) represented a reduction in tracer affinity in response to increase in glutamate. This mechanism requires further investigation since a similar investigation in rhesus monkeys did not replicate this effect (42). One potential mechanism is through increased mGluR5 internalization, which reduces ligand affinity by altering the local intracellular milieu. Regardless of the method by which mGluR5 affinity is decreased, the clinical implication is that this reduced affinity is required for ketamine's downstream effects. This is analogous to our understanding of SSRIs, in which desensitization of the serotonin 1A (5-HT_{1A}) receptor is known to occur after chronic SSRI exposure. Although the mechanism is still unknown, preclinical studies suggest that 5-HT_{1A} internalization may be one process by which this occurs (65, 66). Preclinical studies have also shown that receptors such as 5-HT_{2A} and the Dopamine D2 receptor can experience rapid internalization (67, 68), as may be the case with mGluR5. As such, similar preclinical studies will be needed to fully understand ketamine-induced effects at mGluR5.

The relationship between ketamine-induced effects and mGluR5 binding also needs to be further evaluated. Although ketamine-induced dissociative symptoms were observed in this study, they were not correlated with changes in [^{11}C]ABP688 binding. This is most likely due to the small sample size and the limited range of behavioral score change (due to the fact that these were healthy volunteers). It is also possible that these correlations will only be found after some threshold of V_T change is observed. In this study, seven subjects

experienced <20% change in average V_T after ketamine infusion and three subjects experienced >40% change. This makes uncovering correlations challenging. With a greater number of subjects, there will be more data available to examine correlations at higher percent differences.

As mentioned above, mGluR5 dysfunction has been implicated in models of disease, including depression and addiction. In this work, effects of ketamine treatment on mGluR5 were examined. However, in order to fully elucidate the pathways by which these ketamine-induced effects are clinically therapeutic, a greater understanding about both the role of mGluR5 in these diseases and the downstream effects of mGluR5 modulation are required. Imaging studies such as this would be useful for this purpose, both shedding light on pathophysiology as well as potentially aiding in development of novel therapeutics.

Limitations of this study include: (1) Determination of Mechanism. This study is the first to demonstrate an effect of ketamine administration on [^{11}C]ABP688 binding in humans. However, the mechanism by which this binding reduction occurs remains to be determined. For this reason, it is difficult to assess the cause of the inter-subject variation in ketamine response. Although this variation may be due to individual differences in glutamate release following ketamine administration, as has been previously observed (21), further studies are needed to assess this possibility. (2) No placebo group. All of the subjects were aware they were being administered ketamine and of ketamine's effects, and thus their subjective reports may have been influenced accordingly. However, as this study establishes the proof of concept, future studies can be conducted with a placebo group. Further, with the paradigm established, future studies could be performed in a depressed population, in which mGluR5 binding changes can be associated with response (to either ketamine or placebo). (3) Potential dynamic effects of ketamine that alter tracer delivery and washout. The kinetic modeling used assumes equilibrium conditions (60); however, blood pressure and heart rate were transiently elevated during ketamine administration. Further, ketamine has been shown to induce blood flow elevations in frontal regions (70-72), as measured with fMRI, although the reported effect was not large and localized to a few regions. A similar effect was observed in the current study, with a region-dependent increases in tracer delivery (K_1) throughout the brain. Despite this, we did not detect significant changes in clearance between scans. Further, potential ketamine-induced changes (e.g. metabolism) are accounted for using the outcome measure V_T through the use of the metabolite-corrected arterial input function.

In conclusion, we developed a paradigm to measure ketamine-induced changes in [^{11}C]ABP688 binding *in vivo* in human subjects, which may reflect increases in endogenous glutamate. This finding raises the possibility that this pharmaco-PET paradigm may be a useful approach for characterizing changes in regional brain glutamate release, a potentially important new strategy for studying the neurobiology and treatment of neuropsychiatric disorders.

Acknowledgements

We thank the staff at the Yale University PET Center for their help with radiotracer syntheses and related analyses, as well as imaging the subjects. We acknowledge the biostatistical consultation and support from the Biostatistical

Consulting Core at the School of Medicine, Stony Brook University. We also thank Kiriana Morse for her diligent work in updating and editing this manuscript. Support provided by K01 MH092681 (Esterlis), K01MH091354 (DeLorenzo), Yale Center for Clinical Investigation (UL1RR024139; Esterlis, Krystal, Carson, Sanacora, Bloch), Nancy Taylor Foundation (Esterlis); U.S. Department of Veterans Affairs via its support of the VA National Center for PTSD (Krystal, Esterlis, Sanacora); 2P50AA012879 (Krystal).

References

1. Cozzoli DK, Courson J, Caruana AL, Miller BW, Greentree DI, Thompson AB, Wroten MG, Zhang PW, Xiao B, Hu JH, Klugmann M, Metten P, Worley PF, Crabbe JC, Szumlinski KK. Nucleus accumbens mGluR5-associated signaling regulates binge alcohol drinking under drinking-in-the-dark procedures. Alcoholism, clinical and experimental research. 2012; 36:1623–1633.
2. Spooren W, Ballard T, Gasparini F, Amalric M, Mutel V, Schreiber R. Insight into the function of Group I and Group II metabotropic glutamate (mGlu) receptors: behavioural characterization and implications for the treatment of CNS disorders. Behavioural pharmacology. 2003; 14:257–277. [PubMed: 12838033]
3. Akkus F, Ametamey SM, Treyer V, Burger C, Johayem A, Umbricht D, Gomez Mancilla B, Sovago J, Buck A, Hasler G. Marked global reduction in mGluR5 receptor binding in smokers and ex-smokers determined by [11C]ABP688 positron emission tomography. Proceedings of the National Academy of Sciences of the United States of America. 2013; 110:737–742. [PubMed: 23248277]
4. Deschwanden A, Karolewicz B, Feyissa A, Treyer V, Ametamey S, Johayem A, Burger C, Auberson Y, Sovago J, Stockmeier C, Buck A, Hasler G. Reduced Metabotropic Glutamate Receptor 5 Density in Major Depression Determined by [11C]ABP688 PET and Postmortem Study. American Journal of Psychiatry. 2011
5. Price R, Shungu D, Mao X, Nestadt P, Kelly C, Collins K, Murrough J, Charney D, Mathew S. Amino acid neurotransmitters assessed by proton magnetic resonance spectroscopy: relationship to treatment resistance in major depressive disorder. Biol Psychiatry. 2009; 65:792–800. [PubMed: 19058788]
6. Yüksel C, Öngür D. Magnetic resonance spectroscopy studies of glutamate-related abnormalities in mood disorders. Biol Psychiatry. 2010; 68:785–794. [PubMed: 20728076]
7. Gigante A, Bond D, Lafer B, Lam R, Young L, Yatham L. Brain glutamate levels measured by magnetic resonance spectroscopy in patients with bipolar disorder: a meta-analysis. Bipolar Disord. 2012; 14:478–487. [PubMed: 22834460]
8. Paul IA, Skolnick P. Glutamate and depression: clinical and preclinical studies. Ann N Y Acad Sci. 2003; 1003:250–272. [PubMed: 14684451]
9. aan het Rot M, Collins KA, Murrough JW, Perez AM, Reich DL, Charney DS, Mathew SJ. Safety and efficacy of repeated-dose intravenous ketamine for treatment-resistant depression. Biological psychiatry. 2010; 67:139–145. [PubMed: 19897179]
10. Aan Het Rot M, Zarate CA Jr. Charney DS, Mathew SJ. Ketamine for depression: where do we go from here? Biological psychiatry. 2012; 72:537–547. [PubMed: 22705040]
11. Murrough JW, Perez AM, Pillemer S, Stern J, Parides MK, aan het Rot M, Collins KA, Mathew SJ, Charney DS, Iosifescu DV. Rapid and longer-term antidepressant effects of repeated ketamine infusions in treatment-resistant major depression. Biological psychiatry. 2013; 74:250–256. [PubMed: 22840761]
12. Niciu MJ, Luckenbaugh DA, Ionescu DF, Mathews DC, Richards EM, Zarate CA Jr. Subanesthetic dose ketamine does not induce an affective switch in three independent samples of treatment-resistant major depression. Biological psychiatry. 2013; 74:e23–24. [PubMed: 23726512]
13. Murrough JW, Wan LB, Iacoviello B, Collins KA, Solon C, Glicksberg B, Perez AM, Mathew SJ, Charney DS, Iosifescu DV, Burdick KE. Neurocognitive effects of ketamine in treatment-resistant major depression: association with antidepressant response. Psychopharmacology. 2013
14. Murrough JW, Iosifescu DV, Chang LC, Al Jurdi RK, Green CE, Perez AM, Iqbal S, Pillemer S, Foulkes A, Shah A, Charney DS, Mathew SJ. Antidepressant efficacy of ketamine in treatment-resistant major depression: a two-site randomized controlled trial. The American journal of psychiatry. 2013; 170:1134–1142. [PubMed: 23982301]

15. Berman RM, Cappiello A, Anand A, Oren DA, Heninger GR, Charney DS, Krystal JH. Antidepressant effects of ketamine in depressed patients. Biol Psychiatry. 2000; 47:351–354. [PubMed: 10686270]
16. Aan Het Rot M, Zarate CA Jr. Charney DS, Mathew SJ. Ketamine for Depression: Where Do We Go from Here? Biol Psychiatry. 2012
17. Zarate CA Jr. Singh JB, Carlson PJ, Brutsche NE, Ameli R, Luckenbaugh DA, Charney DS, Manji HK. A randomized trial of an N-methyl-D-aspartate antagonist in treatment-resistant major depression. Archives of general psychiatry. 2006; 63:856–864. [PubMed: 16894061]
18. Lorrain D, Baccei C, Bristow L, Anderson J, Varney M. Effects of ketamine and N-methyl-D-aspartate on glutamate and dopamine release in the rat prefrontal cortex: modulation by a group II selective metabotropic glutamate receptor agonist LY379268. Neuroscience. 2003; 117:697–706. [PubMed: 12617973]
19. Moghaddam B, Adams B, Verma A, Daly D. Activation of glutamatergic neurotransmission by ketamine: a novel step in the pathway from NMDA receptor blockade to dopaminergic and cognitive disruptions associated with the prefrontal cortex. The Journal of neuroscience : the official journal of the Society for Neuroscience. 1997; 17:2921–2927. [PubMed: 9092613]
20. Chowdhury GM, Behar KL, Cho W, Thomas MA, Rothman DL, Sanacora G. (1)H-[(1)(3)C]-nuclear magnetic resonance spectroscopy measures of ketamine's effect on amino acid neurotransmitter metabolism. Biological psychiatry. 2012; 71:1022–1025. [PubMed: 22169441]
21. Stone JM, Dietrich C, Edden R, Mehta MA, De Simoni S, Reed LJ, Krystal JH, Nutt D, Barker GJ. Ketamine effects on brain GABA and glutamate levels with 1H-MRS: relationship to ketamine-induced psychopathology. Molecular psychiatry. 2012; 17:664–665. [PubMed: 22212598]
22. Li N, Lee B, Liu RJ, Banasr M, Dwyer JM, Iwata M, Li XY, Aghajanian G, Duman RS. mTOR-dependent synapse formation underlies the rapid antidepressant effects of NMDA antagonists. Science (New York, NY). 2010; 329:959–964.
23. Li N, Liu R, Dwyer J, Banasr M, Lee B, Son H, Li X, Aghajanian G, Duman R. Glutamate N-methyl-D-aspartate Receptor Antagonists Rapidly Reverse Behavioral and Synaptic Deficits Caused by Chronic Stress Exposure. Biological Psychiatry. 2011; 69:754–761. [PubMed: 21292242]
24. Niesters M, Khalili-Mahani N, Martini C, Aarts L, Gerven Jv, Buchem Mv, Dahan A, Rombouts S. Effect of subanesthetic ketamine on intrinsic functional brain connectivity: a placebo-controlled functional magnetic resonance imaging study in healthy male volunteers. Anesthesiology. 117:868–877. [PubMed: 22890117]
25. Scheidegger M, Walter M, Lehmann M, Metzger C, Grimm S, Boeker H, Boesiger P, Henning A, Seifritz E. Ketamine decreases resting state functional network connectivity in healthy subjects: implications for antidepressant drug action. PloS one. 2012; 7:e44799. [PubMed: 23049758]
26. Esterlis I, Hannestad J, Bois F, Sewell R, Tyndale R, Seibyl J, Picciotto M, Laruelle M, Carson R, Cosgrove K. Imaging changes in synaptic acetylcholine availability in living human subjects. JNM. 2013; 54:78–82. [PubMed: 23160789]
27. Frankle W, Cho R, Narendran R, Mason N, Vora S, Litschge M, Price J, Lewis D, Mathis C. Tiagabine increases [11C]flumazenil binding in cortical brain regions in healthy control subjects. Neuropsychopharmacology. 2009; 34:624–633. [PubMed: 18615011]
28. Thompson J, N NU, Slifstein M, Xu X, Kegeles L, Girgis R, Beckerman Y, Harkavy-Friedman J, Gil R, Abi-Dargham A. Striatal dopamine release in schizophrenia comorbid with substance dependence. Mol Psychiatry. 2012 Epub ahead of print.
29. Narendran R, Jedema H, Lopresti B, Mason N, Gurnsey K, Ruszkiewicz J, Chen C, Deuitch L, Frankle W, Bradberry C. Imaging dopamine transmission in the frontal cortex: a simultaneous microdialysis and [(11)C]FLB 457 PET study. Mol Psychiatry. 2013 Epub ahead of print.
30. Guo N, Guo W, Kralikova M, Jiang M, Schieren I, Narendran R, Slifstein M, Abi-Dargham A, Laruelle M, Javitch JA, Rayport S. Impact of D2 receptor internalization on binding affinity of neuroimaging radiotracers. Neuropsychopharmacology : official publication of the American College of Neuropsychopharmacology. 2010; 35:806–817. [PubMed: 19956086]
31. Sullivan J, Lim K, Labaree D, Lin S, McCarthy T, Seibyl J, Tamagnan G, Huang Y, Carson R, Ding Y, Morris E. Kinetic analysis of the metabotropic glutamate subtype 5 tracer [(18)F]FPEB in

bolus and bolus-plus-constant-infusion studies in humans. J Cereb Blood Flow Metab. 2013; 33:532–541. [PubMed: 23250105]

32. Wong D, Waterhouse R, Kuwabara H, Kim J, Braši J, Chamroonrat W, Stabins M, Holt D, Dannals R, Hamill T, Mozley P. 18F-FPEB, a PET radiopharmaceutical for quantifying metabotropic glutamate 5 receptors: a first-in-human study of radiochemical safety, biokinetics, and radiation dosimetry. J Nucl Med. 2013; 54:388–396. [PubMed: 23404089]
33. DeLorenzo C, Kumar JD, Mann J, Parsey R. *In vivo* variation in metabotropic glutamate receptor subtype 5 binding using positron emission tomography and [^{11}C]ABP688. Journal of Cerebral Blood Flow & Metabolism. 2011; 31:2169–2180. [PubMed: 21792244]
34. Miyake N, Skinbjerg M, Easwaramoorthy B, Kumar D, Girgis R, Xu X, Slifstein M, Abi-Dargham A. Imaging changes in glutamate transmission in vivo with the metabotropic glutamate receptor 5 tracer [11C] ABP688 and N-acetylcysteine challenge. Biological Psychiatry. 2011; 69:822–824. [PubMed: 21288506]
35. Burger C, Deschwanden A, Ametamey S, Johayem A, Mancosu B, Wyss M, Hasler G, Buck A. Evaluation of a bolus/infusion protocol for 11C-ABP688, a PET tracer for mGluR5. Nuclear medicine and biology. 2010; 37:845–851. [PubMed: 20870160]
36. Tsujikawa T, Lyoo C, Siméon F, SZoghbi, Zhang Y, Kimura Y, Pike V, Innis R, Fujita M. Metabotropic glutamate subtype 5 receptors are quantified in human brain with a novel ligand 11C-SP203. SNMMI oral prsentation. 2013
37. Hamilton M. A rating scale for depression. J Neurol Neurosurg Psychiatry. 1960; 23:56–62. [PubMed: 14399272]
38. Montgomery SA, Asberg M. A new depression scale designed to be sensitive to change. The British journal of psychiatry : the journal of mental science. 1979; 134:382–389. [PubMed: 444788]
39. Beck S, Ward C, Mendelsohn M, Erbaugh J. An inventory for measuring depression. Arch Gen Psychiatry. 1961; 4:561–571. [PubMed: 13688369]
40. Bremner J, Krystal J, Putnam F, Southwick S, Marmar C, Charney D, Mazure C. Measurement of dissociative states with the Clinician-Administered Dissociative States Scale (CADSS). J Trauma Stress. 1999; 11:125–136. [PubMed: 9479681]
41. Norcross J, Guadagnoli E, Prochaska J. Factor structure of the profile of mood states (POMs), two partial replications. J Clin Psychol. 1984; 40:1270–1277. [PubMed: 6490926]
42. Sandiego CM, Nabulsi N, Lin SF, Labaree D, Najafzadeh S, Huang Y, Cosgrove K, Carson RE. Studies of the metabotropic glutamate receptor 5 radioligand [(1)(1)C]ABP688 with N-acetylcysteine challenge in rhesus monkeys. Synapse. 2013; 67:489–501. [PubMed: 23424090]
43. Kawamura K, Yamasaki T, Kumata K, Furutsuka K, Takei M, Wakizaka H, Fujinaga M, Kariya K, Yui J, Hatori A, Xie L, Shimoda Y, Hashimoto H, Hayashi K, Zhang MR. Binding potential of (E)-[(11)C]ABP688 to metabotropic glutamate receptor subtype 5 is decreased by the inclusion of its (11)C-labelled Z-isomer. Nuclear medicine and biology. 2014; 41:17–23. [PubMed: 24183615]
44. DeLorenzo C, Milak MS, Brennan KG, Kumar JS, Mann JJ, Parsey RV. In vivo positron emission tomography imaging with [(11)C]ABP688: binding variability and specificity for the metabotropic glutamate receptor subtype 5 in baboons. Eur J Nucl Med Mol Imaging. 2011; 38:1083–1094. [PubMed: 21279350]
45. Treyer V, Streffer J, Wyss MT, Bettio A, Ametamey SM, Fischer U, Schmidt M, Gasparini F, Hock C, Buck A. Evaluation of the metabotropic glutamate receptor subtype 5 using PET and 11C-ABP688: assessment of methods. J Nucl Med. 2007; 48:1207–1215. [PubMed: 17574984]
46. Carson, RE.; Barker, WC.; Liow, J-S.; Johnson, CA. Nuclear Science Symposium Conference Record, 2003. IEEE; 2003. Design of a motion-compensation OSEM list-mode algorithm for resolution-recovery reconstruction for the HRRT.; p. 3281--3285.
47. Anticevic A, Gancsos M, Murray J, Repovs G, Driesen N, Ennis D, Niciu M, Morgan P, Surti T, Bloch M, Raman R, Smith M, Wang X-J, Krystal J, Corlett P. NMDA Receptor Function in Large-Scale Anti-Correlated Neural Systems with Implications for Cognition and Schizophrenia. Proceedings of the National Academy of Science. 2012; 109:16720–16725.
48. Driesen NR, McCarthy G, Bhagwagar Z, Bloch M, Calhoun V, D'Souza DC, Gueorguieva R, He G, Ramachandran R, Suckow RF, Anticevic A, Morgan PT, Krystal JH. Relationship of resting

brain hyperconnectivity and schizophrenia-like symptoms produced by the NMDA receptor antagonist ketamine in humans. Molecular psychiatry. 2013; 18:1199–1204. [PubMed: 23337947]

49. Krystal JH, Karper LP, Seibyl JP, Freeman GK, Delaney R, Bremner JD, Heninger GR, Bowers MB Jr. Charney DS. Subanesthetic effects of the noncompetitive NMDA antagonist, ketamine, in humans. Psychotomimetic, perceptual, cognitive, and neuroendocrine responses. Archives of general psychiatry. 1994; 51:199–214. [PubMed: 8122957]
50. Newcomer JW, Farber NB, Jevtovic-Todorovic V, Selke G, Melson AK, Hershey T, Craft S, Olney JW. Ketamine-induced NMDA receptor hypofunction as a model of memory impairment and psychosis. Neuropsychopharmacology : official publication of the American College of Neuropsychopharmacology. 1999; 20:106–118. [PubMed: 9885791]
51. Oye I, Paulsen O, Maurset A. Effects of ketamine on sensory perception: evidence for a role of N-methyl-D-aspartate receptors. The Journal of pharmacology and experimental therapeutics. 1992; 260:1209–1213. [PubMed: 1312163]
52. Neumeister A, Normandin MD, Murrough JW, Henry S, Bailey CR, Luckenbaugh DA, Tuit K, Zheng MQ, Galatzer-Levy IR, Sinha R, Carson RE, Potenza MN, Huang Y. Positron emission tomography shows elevated cannabinoid CB (1) receptor binding in men with alcohol dependence. Alcoholism, clinical and experimental research. 2012; 36:2104–2109.
53. Rusjan PM, Wilson AA, Bloomfield PM, Vitcu I, Meyer JH, Houle S, Mizrahi R. Quantitation of translocator protein binding in human brain with the novel radioligand [18F]-FEPPA and positron emission tomography. Journal of cerebral blood flow and metabolism : official journal of the International Society of Cerebral Blood Flow and Metabolism. 2011; 31:1807–1816.
54. Gallezot JD, Nabulsi N, Neumeister A, Planeta-Wilson B, Williams WA, Singhal T, Kim S, Maguire RP, McCarthy T, Frost JJ, Huang Y, Ding YS, Carson RE. Kinetic modeling of the serotonin 5-HT(1B) receptor radioligand [(11)C]P943 in humans. Journal of cerebral blood flow and metabolism : official journal of the International Society of Cerebral Blood Flow and Metabolism. 2010; 30:196–210.
55. Wu S, Ogden RT, Mann JJ, Parsey RV. Optimal metabolite curve fitting for kinetic modeling of 11C-WAY-100635. J Nucl Med. 2007; 48:926–931. [PubMed: 17504866]
56. DeLorenzo C, Kumar JS, Mann JJ, Parsey RV. In vivo variation in metabotropic glutamate receptor subtype 5 binding using positron emission tomography and [11C]ABP688. Journal of cerebral blood flow and metabolism : official journal of the International Society of Cerebral Blood Flow and Metabolism. 2011; 31:2169–2180.
57. DeLorenzo, C.; Klein, A.; Mikhno, A.; Gray, N.; Zanderigo, F.; Mann, JJ.; Parsey, RV. SPIE Medical Imaging. Florida, USA: 2009. A new method for assessing PET-MRI coregistration.; p. 72592W-72592W-72598.
58. Logan J, Fowler JS, Volkow ND, Wolf AP, Dewey SL, Schlyer DJ, MacGregor RR, Hitzemann R, Bendriem B, Gatley SJ, Christman DR. Graphical analysis of reversible radioligand binding from time-activity measurements applied to [N-11C-methyl]-(-)-cocaine PET studies in human subjects. Journal of cerebral blood flow and metabolism : official journal of the International Society of Cerebral Blood Flow and Metabolism. 1990; 10:740–747.
59. Patel S, Hamill T, Connolly B, Jagoda E, Li W, Gibson R. Species differences in mGluR5 binding sites in mammalian central nervous system determined using in vitro binding with [18F]F-PEB. Nucl Med Biol. 2007; 34:1009–1017. [PubMed: 17998106]
60. Innis RB, Cunningham VJ, Delforge J, Fujita M, Gjedde A, Gunn RN, Holden J, Houle S, Huang SC, Ichise M, Iida H, Ito H, Kimura Y, Koeppe RA, Knudsen GM, Knuuti J, Lammertsma AA, Laruelle M, Logan J, Maguire RP, Mintun MA, Morris ED, Parsey R, Price JC, Slifstein M, Sossi V, Suhara T, Votaw JR, Wong DF, Carson RE. Consensus nomenclature for in vivo imaging of reversibly binding radioligands. Journal of cerebral blood flow and metabolism : official journal of the International Society of Cerebral Blood Flow and Metabolism. 2007; 27:1533–1539.
61. Hirvonen J, Johansson J, Teras M, Oikonen V, Lumme V, Virsu P, Roivainen A, Nagren K, Halldin C, Farde L, Hietala J. Measurement of striatal and extrastriatal dopamine transporter binding with high-resolution PET and [11C]PE2I: quantitative modeling and test-retest reproducibility. Journal of cerebral blood flow and metabolism : official journal of the International Society of Cerebral Blood Flow and Metabolism. 2008; 28:1059–1069.

62. Elmenhorst D, Aliaga A, Bauer A, Rosa-Neto P. Test-retest stability of cerebral mGluR(5) quantification using [(1)(1)C]ABP688 and positron emission tomography in rats. Synapse. 2012; 66:552–560. [PubMed: 22290765]
63. Patel S, Hamill TG, Connolly B, Jagoda E, Li W, Gibson RE. Species differences in mGluR5 binding sites in mammalian central nervous system determined using in vitro binding with [18F]F-PEB. Nuclear medicine and biology. 2007; 34:1009–1017. [PubMed: 17998106]
64. Kågedal M, Cselényi Z, Nyberg S, Raboisson P, Ståhle L, Stenkrona P, Varnäs K, Halldin C, Hooker A, Karlsson M. A positron emission tomography study in healthy volunteers to estimate mGluR5 receptor occupancy of AZD2066 - Estimating occupancy in the absence of a reference region. Neuroimage. 2013 Epud ahead of print.
65. Bouaziz E, Emerit MB, Vodjdani G, Gautheron V, Hamon M, Darmon M, Masson J. Neuronal phenotype dependency of agonist-induced internalization of the 5-HT(1A) serotonin receptor. The Journal of neuroscience : the official journal of the Society for Neuroscience. 2014; 34:282–294. [PubMed: 24381289]
66. Riad M, Rbah L, Verdurand M, Aznavour N, Zimmer L, Descarries L. Unchanged density of 5-HT(1A) autoreceptors on the plasma membrane of nucleus raphe dorsalis neurons in rats chronically treated with fluoxetine. Neuroscience. 2008; 151:692–700. [PubMed: 18166275]
67. Berry SA, Shah MC, Khan N, Roth BL. Rapid agonist-induced internalization of the 5-hydroxytryptamine2A receptor occurs via the endosome pathway in vitro. Molecular pharmacology. 1996; 50:306–313. [PubMed: 8700138]
68. Macey TA, Gurevich VV, Neve KA. Preferential Interaction between the dopamine D2 receptor and Arrestin2 in neostriatal neurons. Molecular pharmacology. 2004; 66:1635–1642. [PubMed: 15361545]
69. Krueger DD, Osterweil EK, Bear MF. Activation of mGluR5 induces rapid and long-lasting protein kinase D phosphorylation in hippocampal neurons. Journal of molecular neuroscience : MN. 2010; 42:1–8. [PubMed: 20177824]
70. Breier A, Malhotra A, Pinals D, Weisenfeld N, Pickar D. Association of ketamine-induced psychosis with focal activation of the prefrontal cortex in healthy volunteers. Am J Psychiatry. 1997; 154:805–811. [PubMed: 9167508]
71. Vollenweider F, Leenders K, Scharfetter C, Antonini A, Maguire P, Missimer J, Angst J. Metabolic hyperfrontality and psychopathology in the ketamine model of psychosis using positron emission tomography (PET) and [18F]fluorodeoxyglucose (FDG). Eur Neuropsychopharmacol. 1997; 7:9–24. [PubMed: 9088881]
72. Rowland L, Beason-Held L, Tamminga C, Holcomb H. The interactive effects of ketamine and nicotine on human cerebral blood flow. Psychopharmacology. 2010; 208:575–584. [PubMed: 20066400]
73. Ardekani BA, Guckemus S, Bachman A, Hoptman MJ, Wojtaszek M, Nierenberg J. Quantitative comparison of algorithms for inter-subject registration of 3D volumetric brain MRI scans. J Neurosci Methods. 2005; 142:67–76. [PubMed: 15652618]
74. Holmes CJ, Hoge R, Collins L, Woods R, Toga AW, Evans AC. Enhancement of MR images using registration for signal averaging. J Comput Assist Tomogr. 1998; 22:324–333. [PubMed: 9530404]

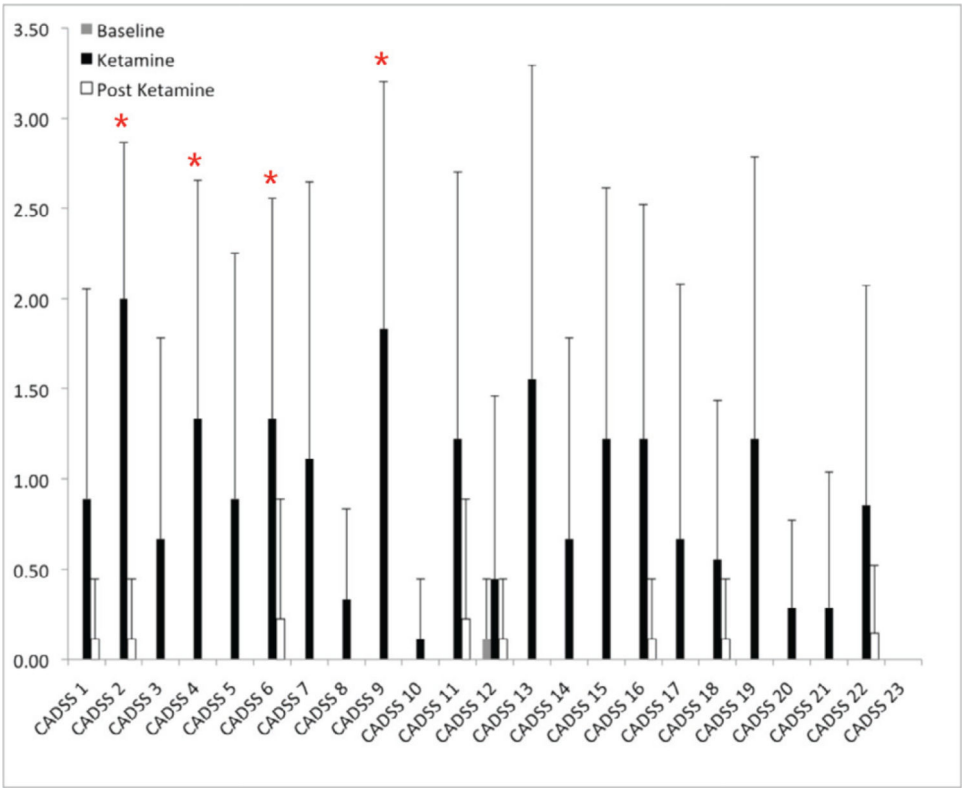

Figure 1.

Average Clinician Administered Dissociative State Scale (CADSS) subscale scores at baseline (before scan 1), during and after the ketamine challenge scan. These assessments were recorded for nine subjects (n=9), except for CADSS 20-23, which were only recorded for seven subjects. Error bars represent the standard deviation in CADSS subscores across subjects. Asterisks represent subscales that were significantly different ($p < 0.05$, uncorrected) between baseline and during the ketamine scan. (With FDR correction all marked subscales had $p < 0.13$.)

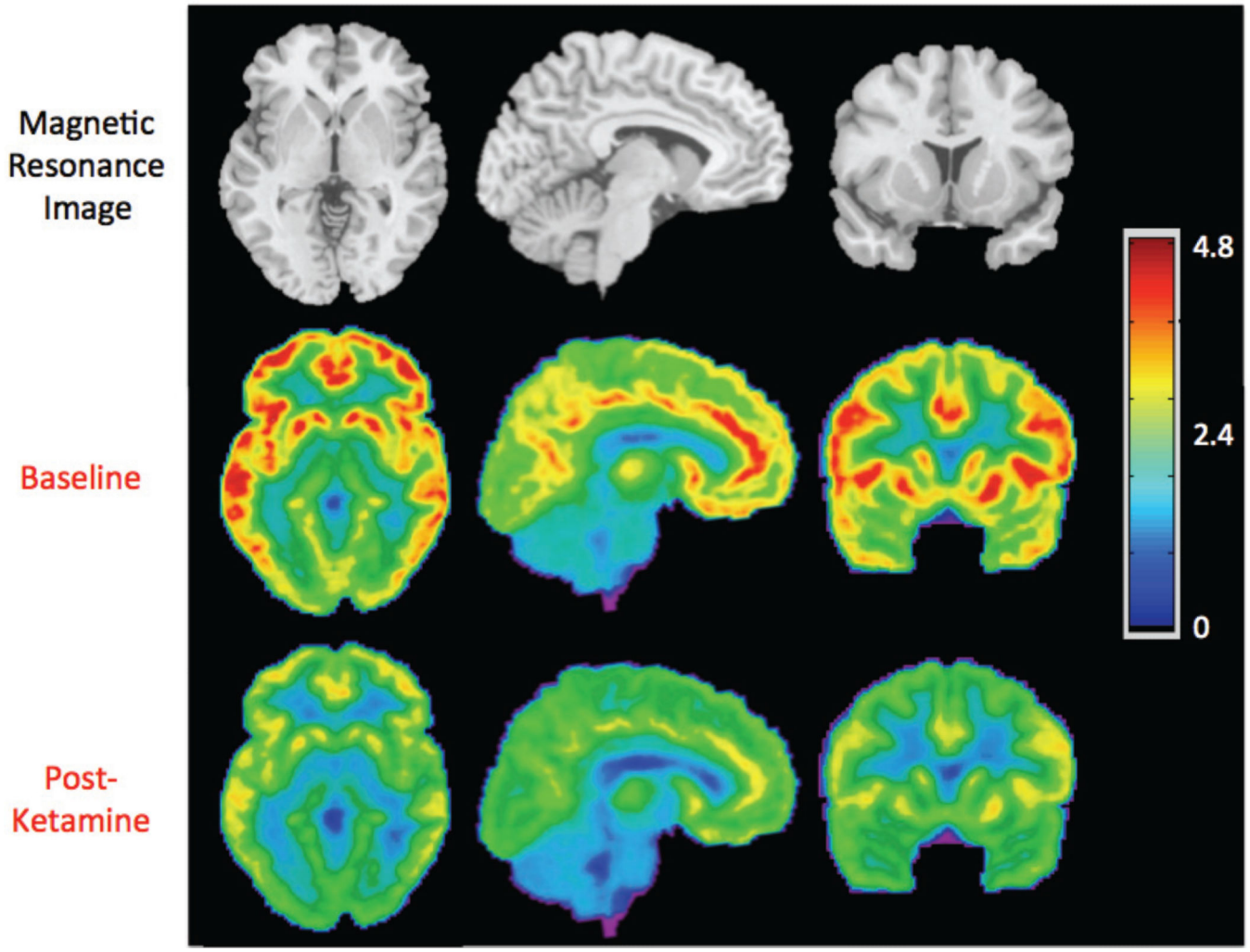

Figure 2.

Average axial, sagittal, and coronal views of [^{11}C]ABP688 binding before and after ketamine administration. For each subject (*n*=10), the volume of distribution (V_T) was calculated at every voxel. These images were warped into standard space using the Automatic Registration Toolbox, ART(73), as previously described.(56) The top row shows the magnetic resonance image template, for anatomical reference.(74) The middle and bottom rows show the corresponding views of the mean [^{11}C]ABP688 V_T image. The V_T value associated with each color is indicated by the color bar.

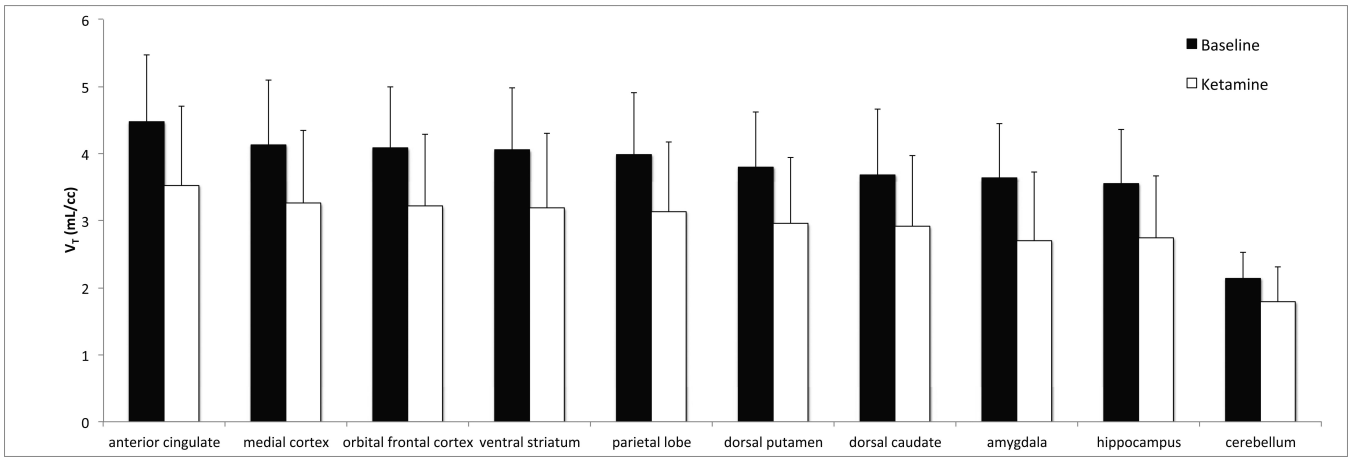

Figure 3.

Average Volume of Distribution (V_T) across subjects (n = 10). Average values during the baseline scans (black bars) and challenge scans (white bars) are shown. Regions are organized from left to right in order of highest to lowest mean baseline binding. Differences in all regions shown are statistically significant ($p<0.05$, uncorrected) in post hoc testing. Error bars represent standard deviation across subjects.

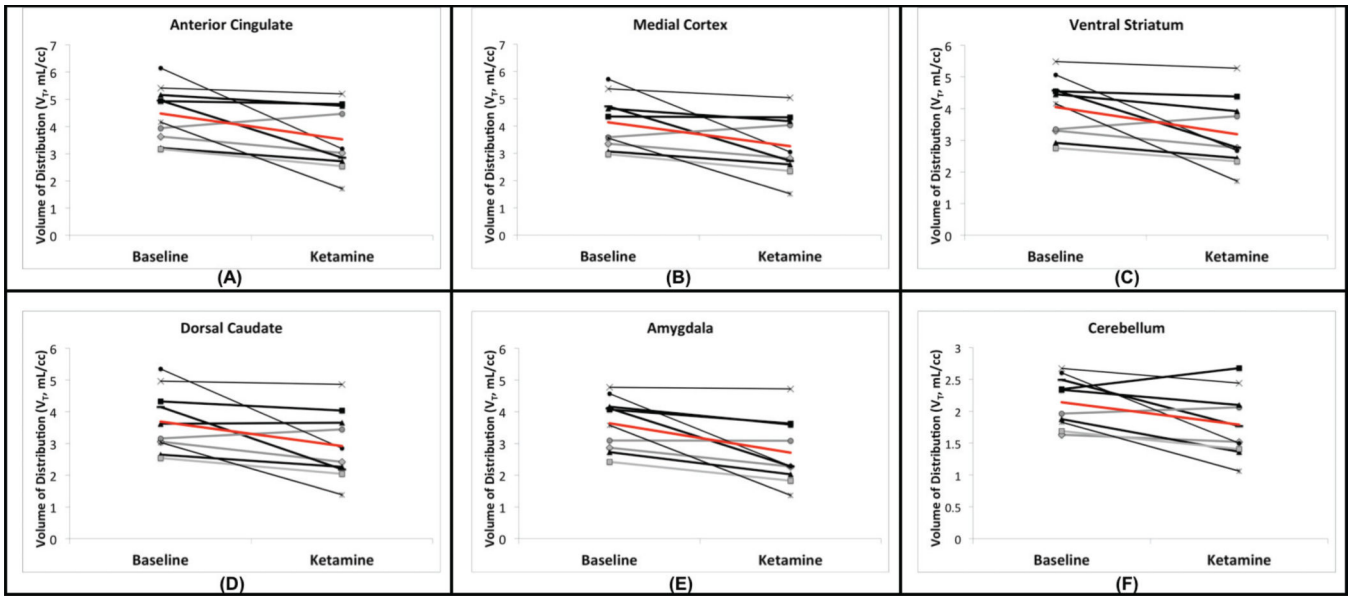

Figure 4.

Effects of Ketamine within each subject. The change in V_T in high (anterior cingulate, a, medial prefrontal cortex, b, and ventral striatum, c) and low (dosal caudate, d, amygdala, e, and cerebellum, f) binding regions is shown. Each line segment represents a different subject. Average change is indicated in red.

Table 1

Mean and standard deviation of subjects' vital signs before and during the ketamine infusion scan.

Min Post Ketamine	Systolic BP	Diastolic BP	Heart Rate	SPO_2 (%)
Baseline	125.9 ± 11.9	63.3 ± 8.4	65.6 ± 11.5	97.5 ± 0.7
4[1]	134.8 ± 23.0	87.2 ± 16.4*	73.3 ± 21.3*	97.9 ± 0.3
9[2]	147.3 ± 26.5*	70.6 ± 11.9*	78.3 ± 16.3*	97.4 ± 1.0
15[2]	139.7 ± 26.1*	70.2 ± 8.7*	77.3 ± 16.8*	97.8 ± 0.7[4]
20[3]	138.7 ± 15.4*	75.6 ± 16.9*	70.8 ± 11.5	97.5 ± 1.2[4]
25[2]	133.4 ± 17.2	69.9 ± 10.3*	75 ± 20.1*	97.5 ± 0.8[4]
30	134.8 ± 17.1	68.9 ± 8.8*	73.1 ± 14.5*	97 ± 1.1[4]
40[2]	130.8 ± 16.5	65.9 ± 7.2	65.1 ± 11.4	97.4 ± 1.2
50	131.4 ± 14.3	68 ± 8.3	66.2 ± 12.7	97.4 ± 1.0
60[2]	133.8 ± 14.2	68.9 ± 6.1*	65.8 ± 12.6	97.7 ± 0.7
75	134.9 ± 16	68.3 ± 7.5	68 ± 12.5	97.8 ± 1.1
90	133.8 ± 19.7	68.4 ± 9.8	70.4 ± 9.4	97.8 ± 0.9

BP: blood pressure. SPO_2: oxygen saturation.

*Using two-tailed t-tests based on a linear mixed model for longitudinal data, these values were significantly different from baseline at an FDR of 10%.

[1]Third subject is missing all measurements at this time.

[2]First subject is missing all measurements at this time.

[3]Ninth subject is subject is missing all measurements at this time.

[4]Seventh subject is missing SPO_2 measurements at these times.

Table 2

Mean and standard deviation for ratings acquired before, during and after (60 min post) the ketamine scan.

	Baseline	During Ketamine Scan	Post Ketamine Scan
CADSS (Amnesia, *n* = 9)	0.0 ± 0.0	5.3 ± 3.9*	0.2 ± 0.7
CADSS (Depersonalization, *n* = 9)	0.1 ± 0.3	12.1 ± 7.1*	0.8 ± 2.3
CADSS (Derealization, *n* = 9)	1.1 ± 1.6	0.1 ± 0.3*	0.9 ± 1.6
POMS T	0.0 ± 0.0	0.3 ± 0.7	0.2 ± 0.6
POMS D	0.6 ± 1.6	0.7 ± 4.3	0.5 ± 1.1
POMS A	1.6 ± 2.4	4.3 ± 4.5	3.3 ± 4.5
POMS F	3.2 ± 1.1	4.5 ± 5.2	3.9 ± 2.0
POMS C	4.4 ± 2.5	5.2 ± 7.7	5.1 ± 4.7
POMS V	2.2 ± 6.4	7.7 ± 1.5	4.2 ± 11.1
POMS Total	3.1 ± 4.4	1.5 ± 0.0	0.9 ± 1.7
BDI	0.0 ± 0.0		3 ± 3.5
HAM-D	0.6 ± 1.1		0.9 ± 1.2
MADRS	0.2 ± 0.6		0.0 ± 0.0 (*n* = 3)

Statistics were calculated using all ten subjects, unless otherwise indicated. Baseline ratings were performed prior to the first scan, except in the case of the POMS, which was acquired before the ketamine scan. No significant differences were observed in the POMS, BDI, HAM-D, or MADRS scores at the different intervals.

*Amnesia: p-value=0.035, FDR=12.5%, Depersonalization: p-value=0.009, FDR=8.6%, and Derealization :p-value=0.004, FDR=8.6%. CADSS: Clinician Administered Dissociative State Scale; POMS: Profile of Mood States; BDI: Beck Depression; HAM-D: Hamilton Rating Scale for Depression; MADRS: Montgomery–Åsberg Depression Rating Scale